

JAAS

Accepted Manuscript



This is an *Accepted Manuscript*, which has been through the Royal Society of Chemistry peer review process and has been accepted for publication.

Accepted Manuscripts are published online shortly after acceptance, before technical editing, formatting and proof reading. Using this free service, authors can make their results available to the community, in citable form, before we publish the edited article. We will replace this *Accepted Manuscript* with the edited and formatted *Advance Article* as soon as it is available.

You can find more information about *Accepted Manuscripts* in the [Information for Authors](#).

Please note that technical editing may introduce minor changes to the text and/or graphics, which may alter content. The journal's standard [Terms & Conditions](#) and the [Ethical guidelines](#) still apply. In no event shall the Royal Society of Chemistry be held responsible for any errors or omissions in this *Accepted Manuscript* or any consequences arising from the use of any information it contains.

1
2
3
4
5
6 **1 Hydrogen analysis in diamond-like carbon with glow discharge optical emission spectroscopy**
7
8

9 2

10
11
12 3 Hikari Takahara¹, Ryoya Ishigami², Kenji Kodama¹, Atsushi Kojyo¹, Tatsuya Nakamura³, Yoshihiro

13
14 4 Oka³
15
16

17 5
18
19

20
21 6 ¹Rigaku Corporation, 14-8 Akaoji-cho, Takatsuki, Osaka 569-1146, Japan
22

23
24 7 ²The Wakasa Wan Energy Research Center, 64-52-1, Nagatani, Tsuruga, Fukui 914-0192, Japan
25

26
27 8 ³University of Hyogo, 2167, Shosha, Himeji, Hyogo 671-2280, Japan
28

29 9
30
31

32 10 a) Corresponding Address
33

34
35 11 X-ray Instrument Division
36

37
38 12 Rigaku Corporation
39

40
41 13 14-8, Akaoji-cho, Takatsuki, Osaka, 569-1146, Japan
42

43
44 14 Tel.: +81-72-693-6813
45

46
47 15 E-mail: hikari@rigaku.co.jp
48

49 16
50
51
52
53
54
55
56
57
58
59
60

1
2
3
4
5
6 **Abstract**
7

8
9 Glow discharge-optical emission spectroscopy (GD-OES) was evaluated for hydrogen analysis
10
11 in diamond-like carbon (DLC) films. DLC film samples were prepared using plasma-based
12
13 ion-implantation and deposition method (PBIID). Their hydrogen contents were determined using
14
15 elastic recoil detection analysis (ERDA). The hydrogen intensity obtained by GD-OES increased
16
17 gradually concomitantly with increasing hydrogen contents at the lower hydrogen content region.
18
19 However, the intensity increased drastically at the higher hydrogen content region of more than
20
21 about 30 at%. When the hydrogen contents increased, the correlation between GD-OES hydrogen
22
23 intensity and ERDA hydrogen contents was deviated from the linear relation obtained for
24
25 hydrogen-implanted silicon samples as reference materials. The sputtering rate of the DLC sample
26
27 was found to vary at high H content region. A linear relationship was obtained between the hydrogen
28
29 contents and GD-OES intensities corrected with the sputtering rate of samples.
30
31
32
33
34
35
36
37
38
39
40
41
42
43
44
45
46
47
48
49
50
51
52
53
54
55
56
57
58
59
60

14 Keywords: GD-OES, DLC, ERDA, hydrogen analysis

1. Introduction

Diamond-like carbon (DLC)¹ has various benefits such as high hardness, low coefficient of friction, and gas-barrier property. In fact, DLC film has attracted much attention for use in industrial parts and devices widely, and recently it has been applied particularly to automotive parts and dies.² The DLC film properties depend on its deposition method, condition, and operating environment.^{3,4} Various methods have been applied for industrial and laboratory uses. Chemical vapor deposition (CVD) method employs hydrocarbon gas as a precursor material so that the deposited film is fated to involve hydrogen contents of approximately to 50 at%. In contrast, hydrogen-free DLC film is formed using physical vapor deposition (PVD), which uses solid carbon as a precursor material. The DLC film amorphous-carbon network structure is a mixture of sp^3 and sp^2 hybridized orbitals, which respectively indicative the diamond structure and graphite structures. The intrinsic hydrogen content and sp^3/sp^2 bonding ratio are closely related to the DLC film characteristics. Therefore a few groups have proposed a means of classification to organize DLC film characteristics using these parameters.^{5,6,7}

Quantitative analysis techniques of hydrogen are limited. E.g., x-ray analysis does not work because hydrogen atoms have no core electron to generate x-ray irradiation and LA-ICP-MS is not applicable because of the air moisture in measurement. LIBS requires inert gas atmosphere. Raman spectroscopy, IR spectroscopy, NMR, EELS, SIMS, and TOF-SIMS provide specific structural

1
2
3
4
5
6 1 characterization and estimation of hydrogen contents in DLC films.¹ Nuclear reaction analysis
7
8
9 2 (NRA) and elastic recoil detection analysis (ERDA)^{8,9,10} have been widely used for direct hydrogen
10
11
12 3 quantification in DLC films, though they require special facilities. In ERDA, hydrogen atom is
13
14
15 4 struck out of the target sample using an ion beam radiation and then the hydrogen atom energy is
16
17
18 5 detected using solid state detector. The ERDA method enables us to quantify hydrogen contents
19
20
21 6 without reference materials and obtain the depth profiles in the samples surface. However, the
22
23
24 7 method is not available in common laboratories because of its requirement of an ion-beam facility.
25
26
27 8 For that reason, glow discharge optical emission spectroscopy (GD-OES) has been considered for
28
29
30 9 use as a laboratory method instead.¹¹ GD-OES is an elemental analysis technique for in-depth
31
32
33 10 direction by which the sample sputtering and atomic emission take place simultaneously in an argon
34
35
36 11 plasma atmosphere.¹² The emission intensity is related to the total weight (or total number of atoms)
37
38
39 12 of the element removed per time from the sample material, which enables quantitative analysis.
40
41
42 13 However, for performing quantitative analysis of hydrogen by GD-OES, suitable certified reference
43
44
45 14 materials are under development. Electroplated zinc coatings and carbon-rich hard coating are
46
47
48 15 studied as the potential candidates.¹³ Additionally, gaseous elements, such as hydrogen, nitrogen and
49
50
51 16 oxygen are fast reacting with each other and other elements. They are cautioned for some possibility
52
53
54 17 of redeposition in the inner surface of the anode in general.¹⁴ In case, the elemental spectral lines are
55
56
57 18 missed to some extent and band spectra are observed instead. This could cause matrix dependence in
58
59
60

1
2
3
4
5
6 1 the calibration. Another problem consists of the chemical bonding state and structure in the
7
8
9 2 hydrogen case. If hydrogen exists dissolved in the matrix lattice without proper bonding like a
10
11
12 3 hydrogen storage alloy, the hydrogen atoms could move out fast from the matrix lattice and the
13
14
15 4 sputtering process has an influence on the distribution of hydrogen in the sample. Even though there
16
17
18 5 are such subjects to be solved for performing quantification of hydrogen, GD-OES method has been
19
20
21 6 considered as a practical analysis method for DLC film. The compatibility of GD-OES with ERDA
22
23
24 7 has already been evaluated by two groups for hydrogen quantification of DLC film.^{11, 15} They
25
26
27 8 compared GD-OES results to hydrogen contents by ERDA for numbers of DLC film samples
28
29
30 9 prepared with various processes. The measuring depth region is different between GD-OES and
31
32
33 10 ERDA; the measurable film thickness was estimated to about 300 nm for the ERDA, but it was
34
35
36 11 several tens micrometers for GD-OES. The first group reported that GD-OES hydrogen intensities
37
38
39 12 averaged from the top surface to 300 nm depth showed a roughly linear relationship with ERDA
40
41
42 13 hydrogen contents, though there were several samples deviated from the trend.¹¹ The second group
43
44
45 14 performed a round robin test on DLC characterization method among several industrial technology
46
47
48 15 institutes in Japan.¹⁵ In their report (not published yet), the GD-OES hydrogen intensities showed not
49
50
51 16 linear but quadratic-like relationship between GD-OES H intensities and ERDA hydrogen contents.
52
53
54 17 Because some sort of relationships were found, GD-OES was proposed as a potential technique for
55
56
57 18 quantitative hydrogen analysis in DLC films in the reports.
58
59
60

1 In this study, detailed evaluation of GD-OES method was performed for hydrogen analysis
2 of DLC film. The GD-OES profile was analyzed. Then the intensity results were compared with
3 those obtained using ERDA. Several DLC samples were prepared with less than 300 nm thickness
4 appropriate for the measurable thickness of ERDA. Simultaneously hydrogen-implanted silicon was
5 evaluated as a reference material for quantifying GD-OES results. The idea of hydrogen-implanted
6 silicon for reference material has been reported and accepted in temperature programmed deposition
7 analysis (TPD).¹⁶ We tried to bring it to hydrogen analysis in GD-OES. The implantation condition
8 was controlled to perform 300 nm in the projected range to measure the entire amount of implanted
9 hydrogen using ERDA.

10 11 12 **2. Experimental**

13 DLC films were prepared using plasma-based ion-implantation and deposition (PBIID)
14 method¹⁷. A PBIID system (Kurita Seisakusyo Co., Ltd.) was available for supplying
15 radio-frequency (RF)-pulse plasma generation and negative high-voltage pulse to the substrate
16 together to perform film deposition and ion-implantation simultaneously. The RF supply was set to
17 500W in peak power, 50 μ s pulse duration, 13.56 MHz frequency, with a 2 kHz repetition rate.
18 Negative high voltage pulse from - 1 to - 10 kV, the duration of 5 μ s, and the repetition rate of 2 kHz

1 were applied to the substrate at 50 μs after each RF pulse. A silicon wafer was used as the substrate.
2 Toluene of hydrocarbon gas was used as the precursor gas. The gas pressure was controlled to 0.7 Pa.
3 The flow rate was set to 30 $\text{cm}^3 \text{min}^{-1}$. The uncoated part was left by protecting with a masking tape
4 to evaluate the film thickness using a stylus profilometer as the height gap between the coated and
5 uncoated part.

6 Hydrogen implantation was performed for the silicon wafer ($\langle 100 \rangle$ in crystal orientation) with
7 a H_2^+ source under 30 kV voltage. Then the projected range was estimated to 300 nm with SRIM
8 software based on Monte Carlo calculation method. The target implantation dose was from 5×10^{16} to
9 10^{18} atoms cm^{-2} by adjusting implantation current (20 -24 μA) and operation time (12 -120 min) for
10 the area of $2 \times 2 \text{ cm}^2$. The sample was tilted at an angle of 7° with respect to the perpendicular beam
11 direction to avoid interference by the channel effect.

12 Prepared DLC films and H-implanted Si wafers were measured using glow discharge optical
13 emission spectroscopy (GD-OES) (GDA750; Rigaku Corp./Spectrums). High purity argon
14 (99.9999%) was used as the discharge gas. Radiofrequency power was applied under the following
15 conditions: 600 V in electric voltage and 300 Pa in gas pressure. The measurement spot was 4 mm
16 diameter. Photomultiplier tubes (PMTs) were used as detector. The following emission lines were
17 applied: H 121.57 nm, C 156.14 nm, and Si 251.51 nm. Molecular spectra were measured with a
18 CCD detector from 215 to 770 nm wavelength and 0.05 nm spectral resolution.

1
2
3
4
5
6 1 Elastic recoil detection analysis (ERDA) was taken in the Tandem accelerator beam line at The
7
8
9 2 Wakasa Wan Energy Research Center. ^4He ions with 2.0 MeV were incident at 10° to the sample
10
11
12 3 surface and then the recoiled H atoms are counted by a detector at 20° in a forward direction.
13
14
15 4 Simultaneously the C or Si content was measured using Rutherford backscattering spectrometry
16
17
18 5 (RBS) method. The backscattered He ions were counted using a detector at 150° against the
19
20
21 6 direction of ^4He ion irradiation.
22
23
24
25
26
27
28

29 8 **3. Results and Discussion**

30 9 **3.1. GD-OES and ERDA profile analysis for DLC film**

31
32 10 The DLC film samples were prepared to have various hydrogen contents by adjusting the
33
34
35 11 deposition conditions.¹⁷ In plasma-based ion-implantation and deposition (PBIID) process condition,
36
37
38 12 increasing negative voltage tends to decrease hydrogen content in DLC film. Alternatively the
39
40
41 13 addition of hydrogen into the precursor gas also decreases the hydrogen content. Table I presents the
42
43
44 14 sample name, deposition conditions and the film thickness. Film samples D1 - D9 were deposited
45
46
47 15 below 300 nm, where ERDA can detect the entire depth region. The samples D10 -D15 were
48
49
50 16 prepared with various practical conditions (300 - 500W RF power, 0.7 - 1.0 Pa gas pressure, -5 – -10
51
52
53 17 kV negative high voltage pulse) which were different from the conditions for the series of D1 – D9.
54
55
56 18 The D10 – D15 samples have larger thickness so that only the upper region to 300 nm is expected to
57
58
59
60

1
2
3
4
5
6 contribute to ERDA results.
7
8

9 Figure 1 presents ERDA spectra for the D2 sample. Figure 1(a) displays the yield of recoiled H
10 atoms against the energy. The profile is quantified to the H atomic density as a function of depth
11 from the sample surface based on the simulation result (Fig. 1(b)). The large H content from 0 to
12 about 0.2 μm is assigned to DLC film. The atomic area densities of hydrogen and carbon from the
13 ERDA and RBS fitting results are presented in Table I. The hydrogen content was calculated from
14 the atomic densities of H and C in the fitting result. The hydrogen contents for D1 to D15 samples
15 were determined as given in Table I.
16
17
18
19
20
21
22
23
24
25
26
27
28

29 Figure 2 portrays GD-OES profiles for samples D2 and D13. The C, H and Si intensities are
30 shown as a function of the sputtering time instead of the distance from the surface. The upper region
31 composed of C and H is attributed to DLC film. The increase of Si intensity is attributed to the Si
32 substrate. In the vicinity of Si substrate, the C and H intensities are enhanced before decreasing, as
33 presented clearly in Fig 2(b). This is expected to be the result of the DLC which is influenced by the
34 fact that Si which has higher sputtering yield than C has.¹⁸ Moreover the C intensity shows a
35 periodical motion for D2 sample (Fig. 2(a)). When the film thickness is sufficiently thin to be
36 transparent, a certain emission wavelength can conduct interference through reflection from the
37 substrate. In the case of D13 sample, the periodical motion disappears because of its opacity by
38 greater thickness (Fig. 2(b)). Therefore the C intensity variation is not originated from the
39
40
41
42
43
44
45
46
47
48
49
50
51
52
53
54
55
56
57
58
59
60

1
2
3
4
5
6 1 concentration variation but from the interference of the emission. The enrichment of C and H on the
7
8
9 2 top surface can result from contamination from the environment, though it was not obvious in the
10
11
12 3 ERDA spectra. Although pre-treatment is useful to clean the sample surface in GD-OES
13
14
15 4 measurement generally, it was not used in this study to have the initial sample surface equivalent in
16
17
18 5 ERDA measurement. The depth resolution in the top surface would be better in GD-OES. The
19
20
21 6 averaged hydrogen intensity was calculated from the plateau intensity and background intensity in
22
23
24 7 each profile. For example, in case of D2 sample shown in Fig. 2 (a), the plateau intensity was
25
26
27 8 averaged between 1.0 and 5.8 s and the background intensity averaged between 15 and 30 s was
28
29
30 9 subtracted from it.
31
32
33
34
35

3.2. GD-OES and ERDA profile analysis for H-implanted Si

36
37
38 12 The H-implanted Si samples with various H contents were measured using GD-OES and
39
40
41 13 ERDA similarly to DLC film samples. Table II gives the sample name and target dose hydrogen.
42
43
44 14 ERDA profile for sample S5 is portrayed in Fig. 3. The ERDA profile exhibits a peak for the
45
46
47 15 implanted hydrogen which is distributed from 50 to 300 nm. Another small peak on the top is well
48
49
50 16 resolved for the surface contamination. Table II presents the atomic area density of hydrogen
51
52
53 17 obtained by ERDA. The surface atomic densities were estimated to $5.9 \times 10^{16} - 3.3 \times 10^{17}$ at cm^{-2}
54
55
56 18 excluding the surface contamination for the samples. The surface atomic densities of the samples are
57
58
59
60

1 mostly equivalent to the corresponding target doses less than 1.0×10^{17} at cm^{-2} . But they are likely
2 saturated for the target doses more than 2×10^{17} at cm^{-2} . The atomic density values were converted to
3 atomic contents, assuming that the amounts of H were present in 300 nm depth of Si with theoretical
4 volume density (2.33 g cm^{-3}).

5 Figure 4 presents GD-OES intensity profiles of H and Si for sample S5. The enrichment of H
6 on the top surface from 0 s to 1.5 s could be attributed to contamination from the environment. The
7 H intensity peak around 4 s is attributed to the implanted hydrogen. The peak structure is attributable
8 to the Gaussian distribution because of the intrinsic characteristics of ion implantation. The peaks
9 spread up to about 6 s for all samples. Referring to the ERDA profile (Fig. 3), the point at 6 s was
10 roughly supposed to 300 nm in depth. This was also supported by the erosion rate ($50 - 60 \text{ nm s}^{-1}$),
11 which was estimated from the depth in crater shape after the measurement. Therefore, the peak
12 profile was fitted with a gauss function and the integrated intensity was time-averaged by 6 s for
13 each profile.

15 3.3. Relationship between GD-OES and ERDA results in DLC film and H-implanted Si

16 samples

17 Figure 5 displays the relationship between the H content by ERDA and the averaged H intensity
18 in GD-OES for DLC samples. Because H-implanted Si system has different matrix composition

1
2
3
4
5
6 1 from DLC system, the GD-OES H intensity of H-implanted Si samples was corrected by using the
7
8
9 2 experimental sputtering rate approximately to plot together in Fig. 5, as described below. The
10
11
12 3 sputtering rate was defined as the number of atoms sputtered per unit area and per unit time (at cm^{-2}
13
14
15 4 s^{-1}) where the atomic area density of the matrix element was divided by the sputtering time for
16
17
18 5 convenience. Experimental sputtering rate for H-implanted Si (SR(H-Si)) was estimated to $2.5 \times$
19
20
21 6 10^{17} at $\text{cm}^{-2} \text{s}^{-1}$ assuming 300 nm depth of Si with theoretical volume density (2.33 g cm^{-3} , $4.99 \times$
22
23
24 7 10^{22} at cm^{-3}) is sputtered by 6 s, as shown in Fig. 4. H peak appeared up to 6 s consistently for the
25
26
27 8 H-implanted Si samples in GD-OES profiles and the sputtering time (6 s) taken for the depth of
28
29
30 9 implantation (300 nm) was almost constant for all H-implanted Si samples. Experimental sputtering
31
32
33 10 rate for DLC (SR(DLC)) was estimated based on the data for sample D4 with the least H contents
34
35
36 11 among the D1-D9 series. The area density of C for D4 was 20.5×10^{17} at cm^{-2} by RBS analyses,
37
38
39 12 shown in Table I. The entire film of D4 is sputtered by 16.7 s in GD-OES (not shown). Therefore the
40
41
42 13 experimental sputtering rate for DLC (SR(DLC)) was estimated to 1.23×10^{17} at $\text{cm}^{-2} \text{s}^{-1}$. The
43
44
45 14 SR(H-Si) was high by a factor of 2.0 ($2.5/1.23$) compared to SR(DLC), so that the H intensities
46
47
48 15 obtained for H-implanted Si samples were divided by the factor (2.0) in Fig. 5.

16 Regarding to the H-implanted Si samples, the GD-OES averaged H intensity is linearly
17
18 correlated to ERDA H contents. DLC samples are likely to sustain the linear relation between
19
20
21 18 GD-OES and ERDA at the lower H contents. However, the GD-OES H intensity increased

1 drastically at more than about 30 at% to enhance the increasing slope. The curve shape was not
2 expressed by the first approximation but by kind of a polynomial or exponential function for the
3 wide H content range. Although we considered H-implanted Si samples to serve as reference
4 samples for DLC film analysis, the DLC result differed from the extrapolation of H-implanted Si
5 result more and more with higher H content region.

6 The drastically enhancement of GD-OES H intensity at the high H contents was confirmed if it
7 occurred in association with the emission line choice or sputtering rate variation. The monitored
8 optical emission for H analysis is a resonance line at 121.57 nm. The emission characteristics for the
9 individual line, with characteristics such as excitation, absorption, and detailed energy transfers
10 between energy levels, can affect to the intensity variation. For example, the resonance emission line
11 is well known to tend to be saturated with the contents. Another H emission line at 656.28 nm is a
12 non-resonance and visible line of the Balmer series which is related to different energy levels from
13 121.57 nm. Figure 6 depicts the H emission intensity at 656.28 nm against that at 121.57 nm for
14 DLC film samples. A linear relation appeared between the intensities at 656 nm and 121 nm,
15 suggesting that the incomprehensive increment of H intensity at the high content region would not
16 result from the emission mechanism. In other words, the hydrogen concentration in the plasma
17 would actually increase to raise the H intensity drastically. Figure 7 displays the sputtering rate
18 variation to H contents for the DLC film samples. The sputtering rate was estimated from the

1
2
3
4
5
6 1 number dividing the total area atomic density of H and C by the sputtering time taken for the whole
7
8
9 2 range in each film sample. The sputtering rate of multicomponents is not explained simply but it is
10
11
12 3 likely related with the mass, atomic radius, binding energy, and other characteristics of the
13
14
15 4 constituents in a general sense.¹⁸ According to these authors, the sputtering rate will have the trend
16
17
18 5 of concomitant increase with increasing H contents considering the smaller mass and/or atomic
19
20
21 6 radius. From the characteristics of DLC too, the hydrogen content is closely related to the sp^2/sp^3
22
23
24 7 bonding state, density, and structural hardness. It is well-known that the DLC shows tendency to lose
25
26
27 8 the structural hardness by containing hydrogen in general. The decline of structural hardness could
28
29
30 9 bring the enhancement of sputtering rate and the drastically increase of hydrogen intensity for high
31
32
33 10 H contents of DLC.

34
35 11 The sputtering rate enhancement with increasing hydrogen contents in DLC is also in
36
37
38 12 agreement with the experimental results of the molecular spectra measurements. Figures 8 (a) and
39
40
41 13 (b) respectively depict the molecular spectra of C-H and C-C,^{19,20,21} which were recorded with a
42
43
44 14 spectrometer equipped with a CCD detector in GD-OES tool. The C-H molecular band structure was
45
46
47 15 observed in the wavelength range of 429-432 nm (Fig. 8 (a)). The C-H band intensity increased
48
49
50 16 concomitantly with increasing H contents in DLC samples, which indicates the formation of CH
51
52
53 17 radical. Additionally, C-C band at 510-570 nm is also strong for higher H containing samples. Two
54
55
56 18 peaks of several peaks in the band are exhibited in Fig. 8 (b), which indicates the formation of CC

1 radicals also increased with increase of H contents. Figure 9 depicts the intensity dependence on the
2 H contents by ERDA for H peak at 121.57 nm, C peak at 156.14 nm, a representative C-H peak at
3 430.38 nm and C-C peak at 558.52 nm. The C intensity was almost constant for the H contents, as
4 marked with open circles in Fig. 9, though the C contents decreased instead of increase of H contents.
5 C intensity might be filled by the increase of sputtering rate to have almost constant intensity, further
6 study is necessary to make clear the mechanism. The C-H peak and C-C peak intensities clearly
7 increased with H contents, indicating efficient formation of such fragments by sputtering rate
8 enhancement.

9 However, “hydrogen effect”²², which is well-known in GD-OES analysis, should be considered
10 as a supplement reason for to the intensity relationship with H contents. Hydrogen effect modifies
11 the optical emission intensities accompanied with the existence of hydrogen molecule (H₂). This
12 occurs because metastable state of Ar (Ar^m), which has a large contribution to ionization processes,
13 is quenched by collision with H₂ molecule.^{23,24} Most analytical lines decrease in emission yields,
14 however some lines are selectively excited. Therefore the intensity dependence of C, C-H peak and
15 C-C peak on H contents might be possible. The further theoretical study is necessary to understand if
16 hydrogen effect could contribute to their intensity changes or not.

17 Figure 10 plots the GD-OES H intensity corrected by the sputtering rate against the H contents
18 by ERDA for DLC samples. Mostly linear relation between the corrected intensities and H contents

1
2
3
4
5
6 1 appeared. The sputtering rate variation should be taken into consideration for analyzing hydrogen
7
8
9 2 contents in DLC with GD-OES. Moreover, volatile materials formation, not only of CH and CC but
10
11
12 3 of multiple fragments such as CH₂, CH₃, and C₂H₆ which have poor possibilities for optical emission,
13
14
15 4 is anticipated. Single hydrogen atom emission can be affected if their contributions are too great to
16
17
18 5 ignore. In the lower concentration range below 15 %, further investigation is necessary if the matrix
19
20
21 6 independent calibration of H in Si and C is possible.
22
23
24 7
25
26
27
28

26 8 **Conclusion**

29 9 Hydrogen analysis using GD-OES was evaluated for DLC films. Several DLC film samples
30
31
32 10 were prepared using PBIID method. Their hydrogen contents were determined with ERDA. The
33
34
35 11 hydrogen intensity obtained by GD-OES was compared with the H contents of the sample using
36
37
38 12 ERDA. No linear relationship between them was found in the results: The GD-OES intensity
39
40
41 13 increased with the H content at the hydrogen content region less than 30 at% but increased
42
43
44 14 drastically at the higher H content region. At the higher H content region, the variation in GD-OES
45
46
47 15 H intensity did not correspond to that for H-implanted Si samples which were regarded as reference
48
49
50 16 materials. The sputtering rate of sample, which was estimated from the atomic density and sputtering
51
52
53 17 time, drastically increase for the high H content region. In the molecular spectra, the formation of
54
55
56 18 volatile material fragments such as CH and CC increased for high H content regions. This suggests
57
58
59
60

1
2
3
4
5
6 1 decline of the structural hardness to cause the fast sputtering rate with increase of H contents in DLC
7
8
9 2 samples. By correcting the sputtering rate variation of samples, the GD-OES hydrogen intensity
10
11
12 3 shows linear relationship to the hydrogen contents by ERDA.
13
14
15 4
16
17

18 **Acknowledgements**

19
20
21 6 We thank Yoshimi Nishimura (Kurita Seisakusyo Co., Ltd.) for supplying DLC film samples.
22

23
24 7 We are grateful to Professor Kazuaki Wagatsuma (Tohoku University) for his helpful discussion and

25
26 8 comments related to GD-OES analysis. We are also grateful to Michael Analytis and Rüdiger

27
28
29 9 Meihnsner (Spectruma Analytik GmbH) for their technical support related to GD-OES measurements.
30
31

32 10
33
34
35
36
37
38
39
40
41
42
43
44
45
46
47
48
49
50
51
52
53
54
55
56
57
58
59
60

1
2
3
4
5
6 **1 Figure captions**
7

- 8
9 2 Fig. 1 ERDA spectra for a DLC film sample of D2. The experimental and simulation results are
10
11
12 3 marked respectively with black dots and gray line in energy spectrum of recoil hydrogen (a).
13
14 4 Furthermore the quantified result (b).
15
16
17 5 Fig. 2 GD-OES depth profiles for DLC film samples of D2 (a) and D13 (b).
18
19
20 6 Fig. 3 Quantified ERDA spectrum for H-implanted Si sample of S5.
21
22
23 7 Fig. 4 GD-OES depth profiles for H-implanted Si sample of S5.
24
25
26 8 Fig. 5 Relation between the averaged H intensity at 121.57 nm by GD-OES and the H contents by
27
28
29 9 ERDA for DLC film. For H-implanted Si samples, the GD-OES H intensity was corrected by using
30
31
32 10 experimental difference on sputtering rate. The DLC film sample results were distinguished by the
33
34
35 11 thickness below (filled squares) /above (open squares) 300 nm of the ERDA measuring depth to
36
37
38 12 confirm the dependence of thickness.
39
40
41 13 Fig. 6 Relation between the averaged H intensity at 656.28 nm and 121.57 nm for DLC film
42
43
44 14 samples.
45
46
47 15 Fig. 7 GD-OES sputtering rate dependence on ERDA H composition.
48
49
50 16 Fig. 8 Molecular spectra of CH band (a) and CC band (marked with *) (b) for the DLC samples. The
51
52
53 17 lines masked with gray are assigned to Ar peaks.
54
55
56
57
58
59
60

- 1
2
3
4
5
6 1 Fig. 9 GD-OES intensity dependences on ERDA H contents for C 156.14 nm, H 121.56 nm, CH
7
8
9 2 430.38 nm, and CC 558.50 nm.
10
11
12 3 Fig. 10 Dependence of the H intensity corrected by the sputtering rate on H contents by ERDA for
13
14 4 DLC film samples.
15
16
17
18 5
19
20
21 6
22
23
24
25
26
27
28
29
30
31
32
33
34
35
36
37
38
39
40
41
42
43
44
45
46
47
48
49
50
51
52
53
54
55
56
57
58
59
60

1

2 Table I Deposition condition (negative voltage and hydrogen atmosphere) and film thickness for DLC
3 samples. The film thickness was measured with a stylus profilometer. The area densities of H and C were
4 obtained by ERDA and RBS analysis. The hydrogen content was calculated from the ratio of H to total (H
5 + C) area densities.

Sample	Deposition cond.	Thickness (μm)	H area dens. (10^{17} at cm^{-2})	C area dens. (10^{17} at cm^{-2})	H content (at%)
D1	-1 kV	0.086	3.88	7.13	35.2
D2	-3 kV	0.18	5.84	13.2	30.7
D3	-5 kV	0.20	6.28	16.2	28.0
D4	-10 kV	0.19	5.46	20.5	21.0
D5	-10 kV	0.21	5.63	20.4	21.6
D6	H atmosphere	0.15	3.02	9.68	23.8
D7	H atmosphere	0.08	1.52	5.86	20.6
D8	-1 kV	0.29	9.20	19.7	31.9
D9	-1 kV	0.23	6.71	13.8	32.8
D10	-5 kV	0.73	34.4	79.5	30.2
D11	-10 kV	1.44	32.1	160	16.7
D12	-10 kV	4.12	75.4	337	18.3
D13	-7 kV	2.32	38.5	193	16.6
D14	-10 kV	0.94	16.6	77.4	17.7
D15	-10 kV	2.16	36.3	180	16.8

6

7

8

1

2 Table II Target dose and the area density obtained ERDA analysis for H-implanted Si sample. H content
3 was calculated from the area density, assuming that H presented in 300 nm depth of Si with theoretical
4 volume density (2.33 g cm^{-3}).

5

6

7

Sample	Target dose H ($10^{17} \text{ at cm}^{-2}$)	H area dens. ($10^{17} \text{ at cm}^{-2}$)	H content (at%)
S1	10	3.35	18.4
S2	5	2.62	15.0
S3	1	1.07	6.7
S4	0.5	0.54	3.5
S5	2	1.60	9.7
S6	1	1.05	6.6
S7	0.5	0.59	3.8
S8	5	3.00	16.8

8

9

10

11

12

13

14

15

16

17

18

19

20

21

22

23

24

25

26

27

28

29

30

31

32

33

34

35

36

37

38

39

40

41

42

43

44

45

46

47

48

49

50

51

52

53

54

55

56

57

58

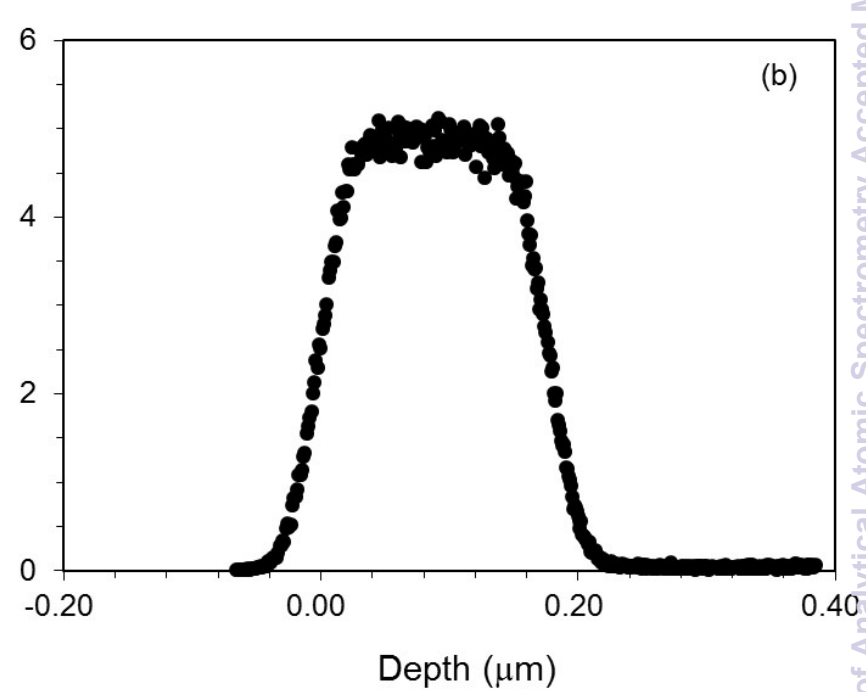
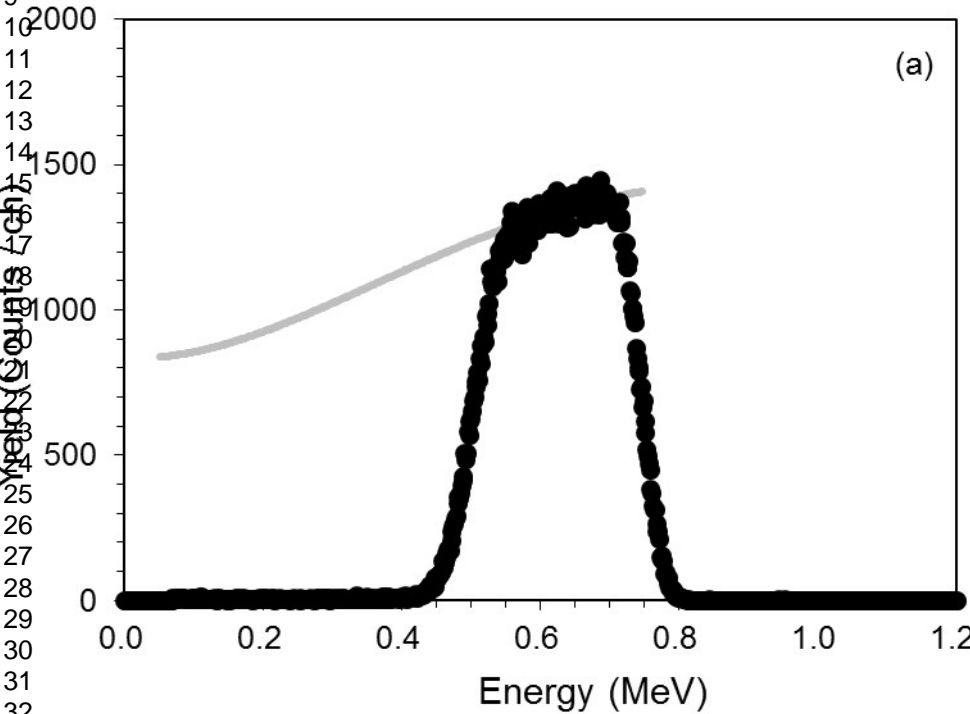
59

60

1

- ¹ J. Robertson, *Materials Science and Engineering*, 2002, **R 37**, 129.
- ² J. Vetter, *Surface and Coating Technology*, 2014, **257**, 213.
- ³ C. Donnet, J. Fontaine, A. Grill, and T. Le Mogne, *Tribology Letters*, 2000, **9**, 137.
- ⁴ A. Grill, *Diamond and Related Materials*, 1999, **8**, 428.
- ⁵ W. Jacob and W. Muller, *Appl. Phys. Lett.*, 1993, **63**, 1771.
- ⁶ A. C. Ferrari and J. Robertson, *Phys. Rev. B*, 2000, **61**, 14095.
- ⁷ H. Saitoh, *J. J. Appl. Phys.*, 2012, **51**, 090120.
- ⁸ M. Cekada, M. Kahn, P. Pelicon, Z. Siketic, I. Bogdanovic, W. Waldhauser, and S. Paskvale, *Surface and Coating Technology* 2012, **211**, 72.
- ⁹ Y. Konishi, I. Konishi, N. Sakauchi, S. Hayashi, A. Hiramoto, and J. Suzuki, *Nuclear Instruments and Methods in Physics Research B*, 1996, **118**, 312.
- ¹⁰ K. Yasuda, C. Batchuluun, R. Ishigami, and S. Hibi, *Nuclear Instruments and Methods in Physics Research B*, 2011, **269**, 1019.
- ¹¹ T. Saitoh, *New Diamond*, 2012, **28**, 27 (in Japanese).
- ¹² M. Winchester and R. Payling, *Spectrochimica Acta B*, 2004, **59**, 607.
- ¹³ V. D. Hodoroba, D. Klemm, U. Reinholz, E. Strub, J. Rohrich, W. Bohne, V. Hoffmann, and K. Wetzig, *J. Anal. At. Spectrom.*, 2008, **23**, 460.
- ¹⁴ Z. Weiss, *Spectrochimica Acta B*, 2006, **61**, 121.
- ¹⁵ K. Baba (2013), "DLC films and round robin test among Japanese industrial technology institutes", paper presented in 38th dry coating study group, Amagasaki ARIC building, Hyogo (in Japanese).
- ¹⁶ N. Hirashita, T. Jimbo, T. Matsunaga, M. Matsuura, M. Morita, I. Nishiyama, M. Nishizuka, H. Okumura, A. Shimazaki, and N. Yabumoto, *J. Vac. Sci. Technol.*, 2001, **A19(4)**, 1255.
- ¹⁷ Y. Oka, M. Nishijima, K. Hiraga, and M. Yatsuzuka, *IEEE Transaction of Plasma Science*, 2006, Vol. 34, No. 4, 1183.
- ¹⁸ D. Fang and R. K. Marcus, *Glow Discharge Spectroscopies*, R. K. Marcus, Editor, p.30-31, Plenum Press, New York (1993).
- ¹⁹ H. Takahara, A. Kojyo, K. Kodama, T. Nakamura, K. Shono, Y. Kobayashi, M. Shikano, and H. Kobayashi, *J. Anal. At. Spectrom.*, 2014, **29**, 95.
- ²⁰ A. Bengtson, *J. Anal. At. Spectrom.*, 2003, **18**, 1066.
- ²¹ R. W. B. Pearse, and A. G. Gaydon, *The Identification of Molecular Spectra*, Chapman and Hall, London, 1976.
- ²² A. Martine, A. Menendez, R. Pereiro, N. Bordel, and A. Sanz-Medel, *Anal. Bioanal. Chem.*, 2007, **388**, 1573.
- ²³ V. D. Hodoroba, V. Hoffmann, E. B. M. Steers, and K. Wetzig, *J. Anal. At. Spectrom.*, 2000, **15**, 951.
- ²⁴ A. Bogaerts, *Spectrochimica Acta*, 2009, **B 64**, 1266.

1
2
3
4
5
6
7
8
9
10
11
12
13
14
15
16
17
18
19
20
21
22
23
24
25
26
27
28
29
30
31
32
33
34
35
36
37
38
39
40
41
42



Journal of Analytical Atomic Spectrometry Accepted Manuscript

Fig1

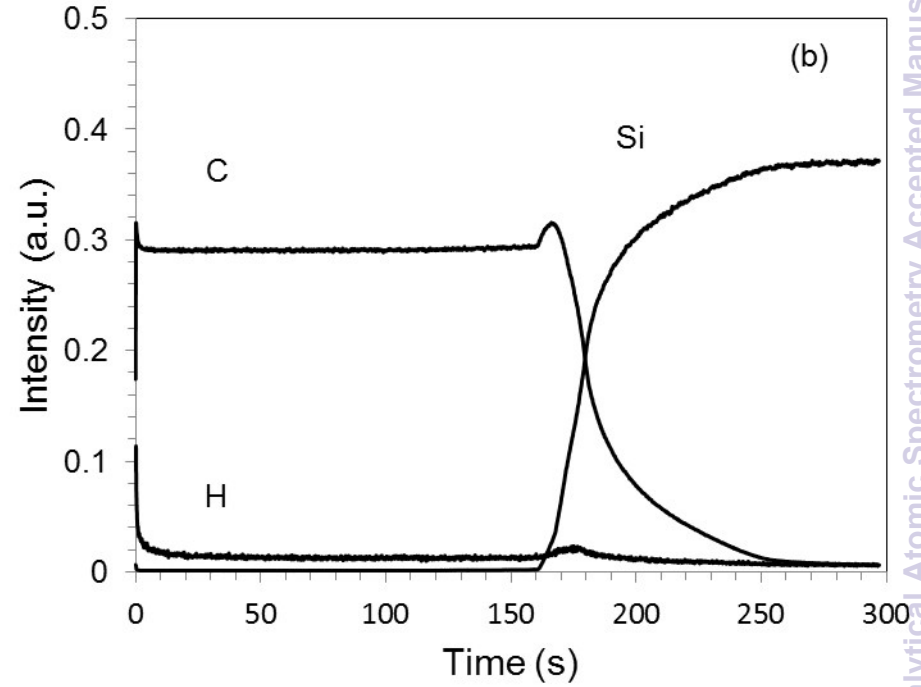
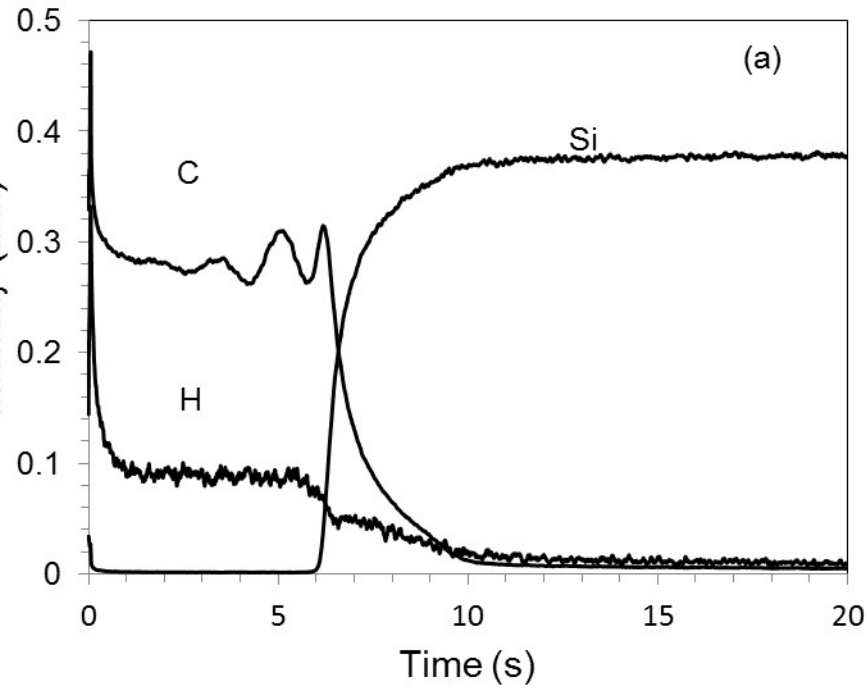
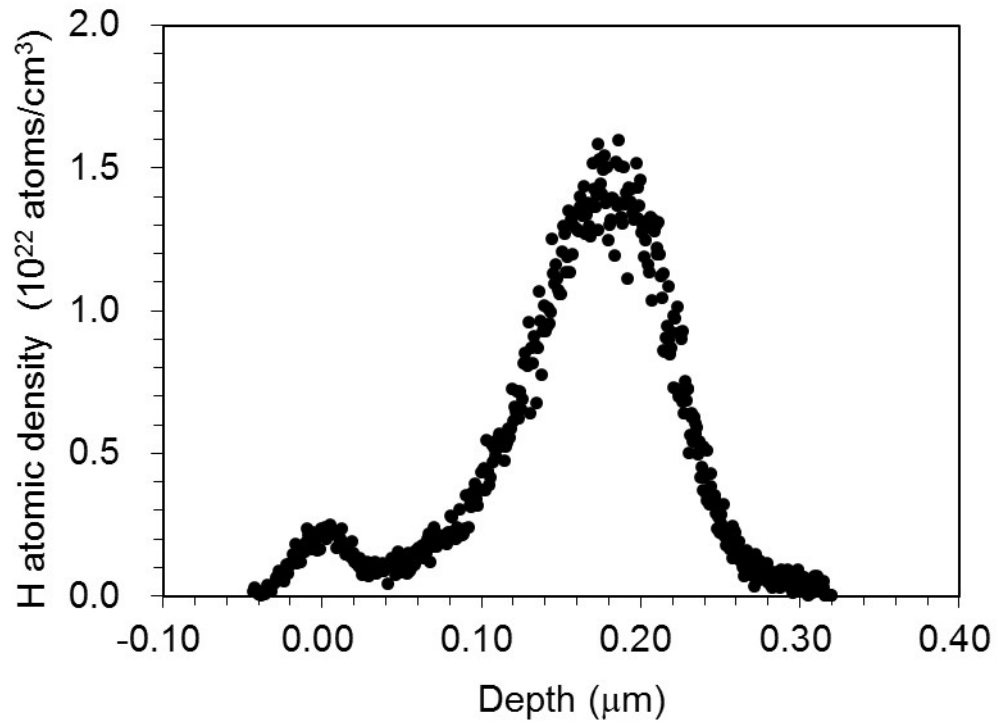
1
2
3
4
5
6
7
8
9
10
11
12
13
14
15
16
17
18
19
20
21
22
23
24
25
26
27
28
29
30
31
32
33
34
35
36
37
38
39
40
41
42
43

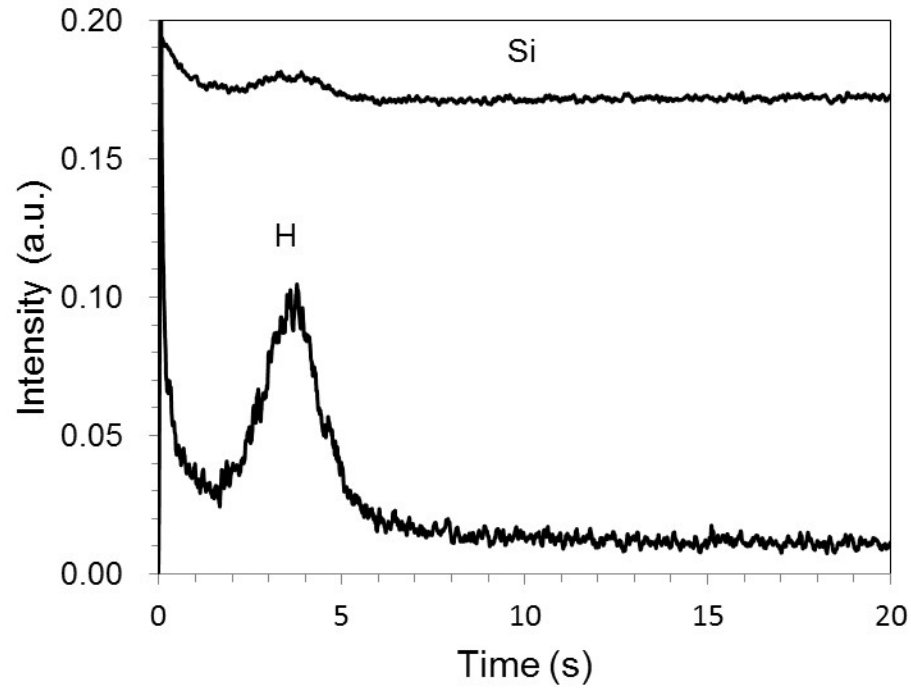
Fig2

1
2
3
4
5
6
7
8
9
10
11
12
13
14
15
16
17
18
19
20
21
22
23
24
25
26
27
28
29
30
31
32
33
34
35
36
37
38
39
40
41
42
43

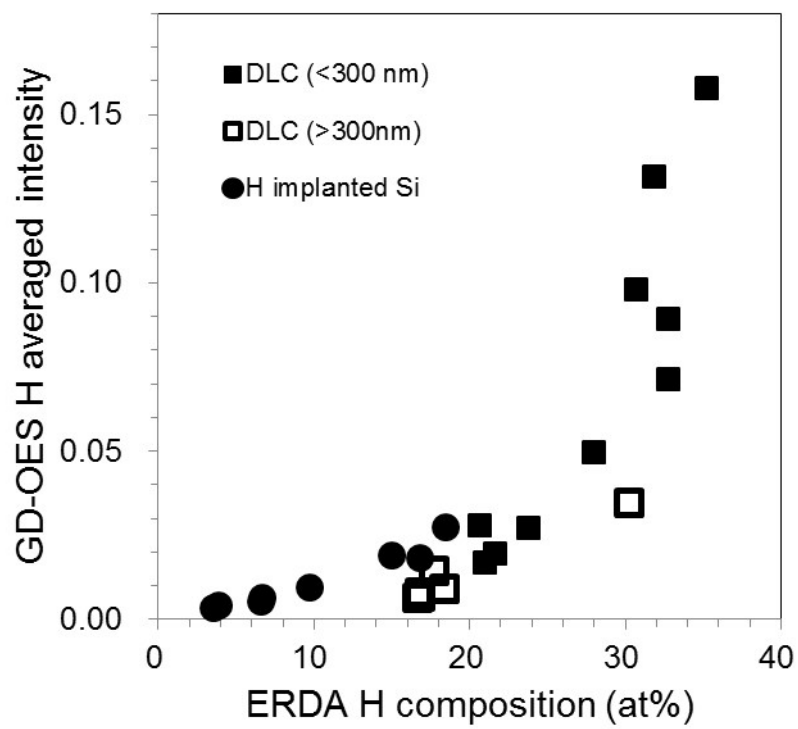


Journal of Analytical Atomic Spectrometry Accepted Manuscript

Fig3

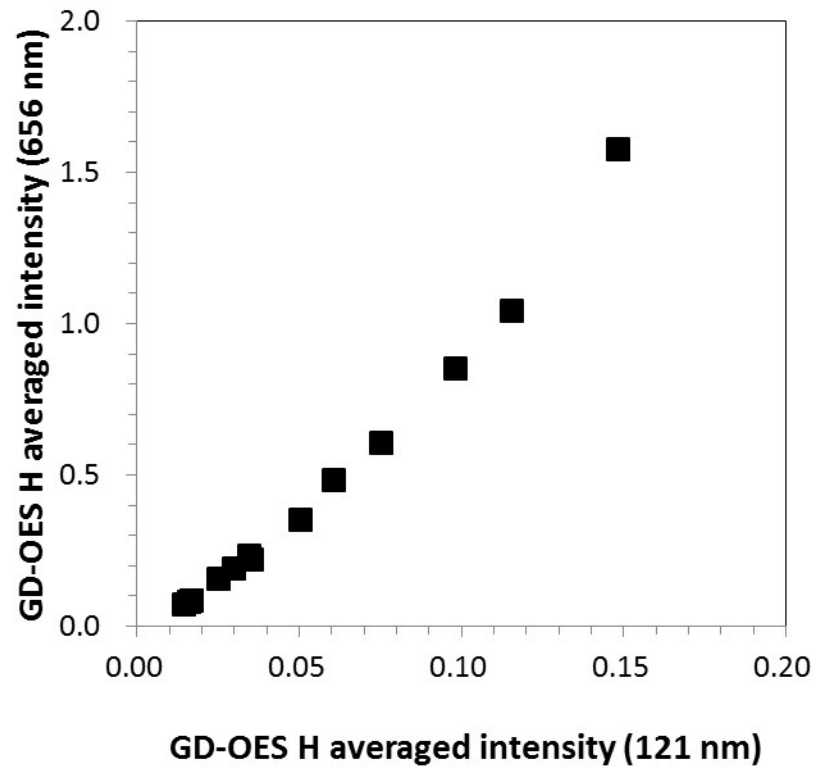


1
2
3
4
5
6
7
8
9
10
11
12
13
14
15
16
17
18
19
20
21
22
23
24
25
26
27
28
29
30
31
32
33
34
35
36
37
38
39
40
41
42
43

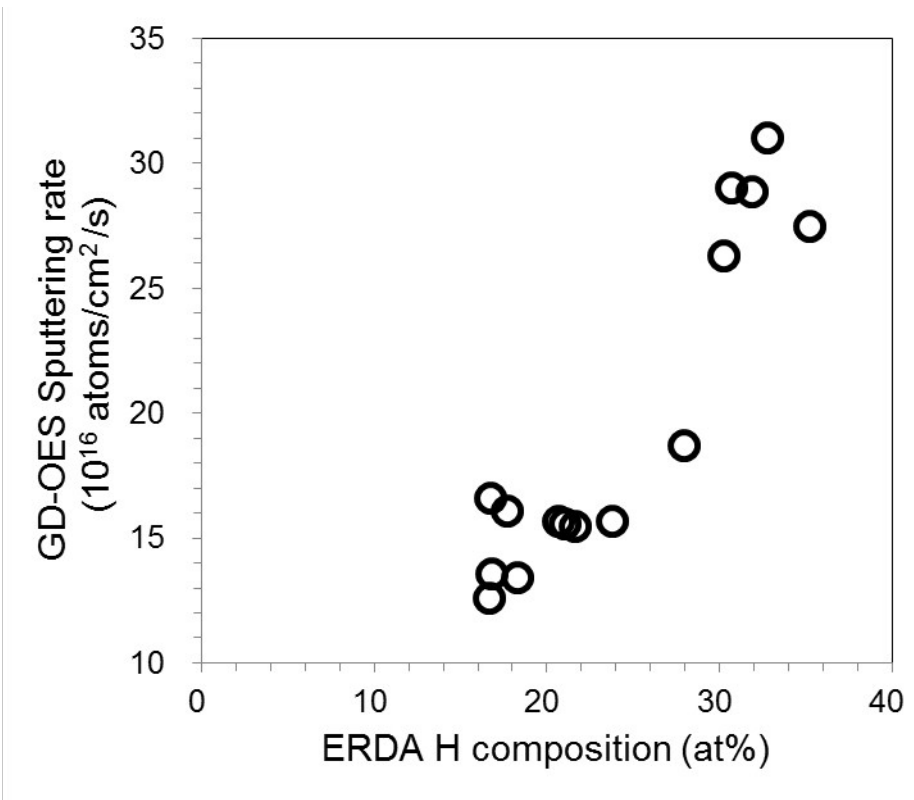


Journal of Analytical Atomic Spectrometry Accepted Manuscript

Fig5

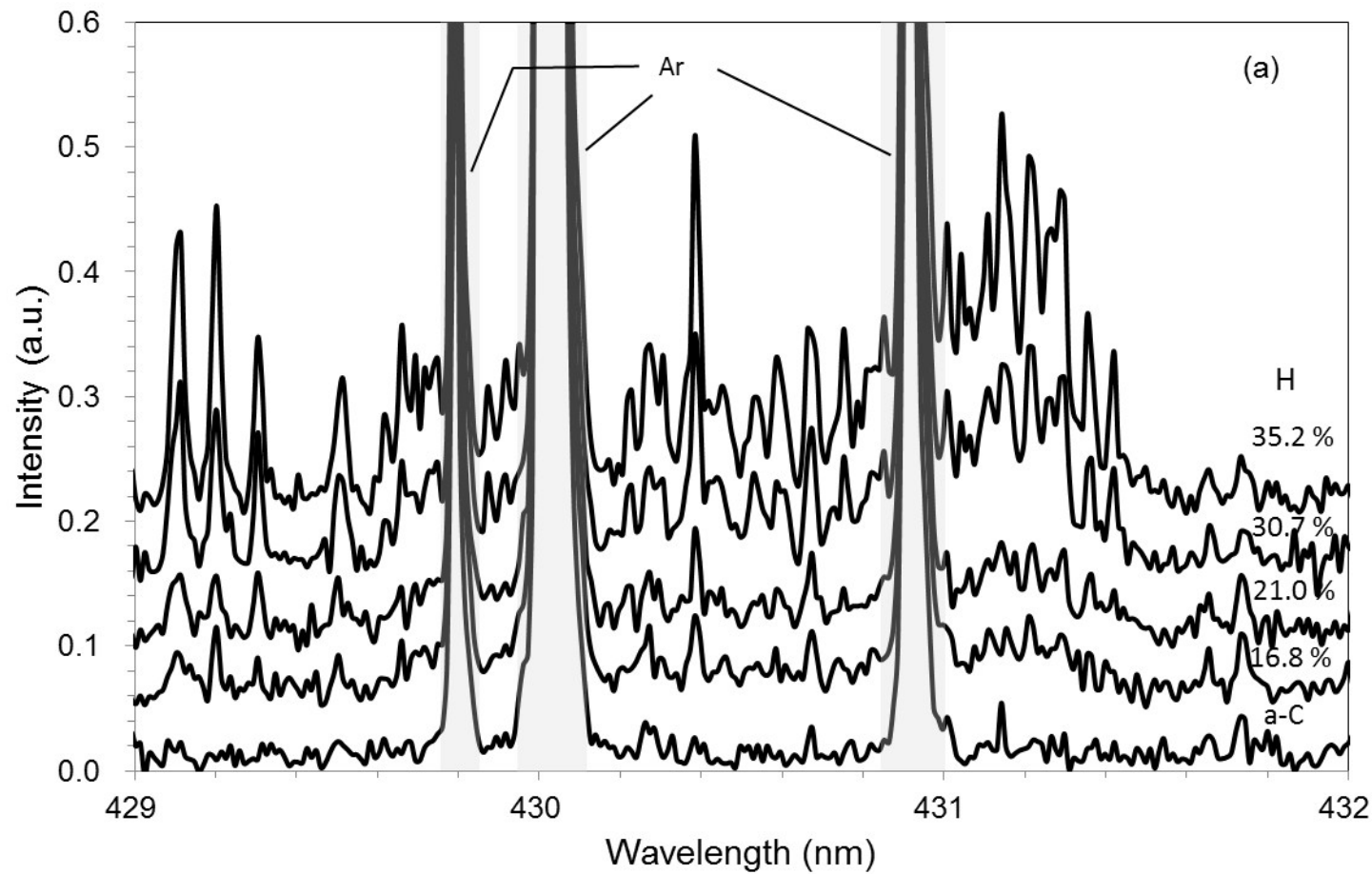


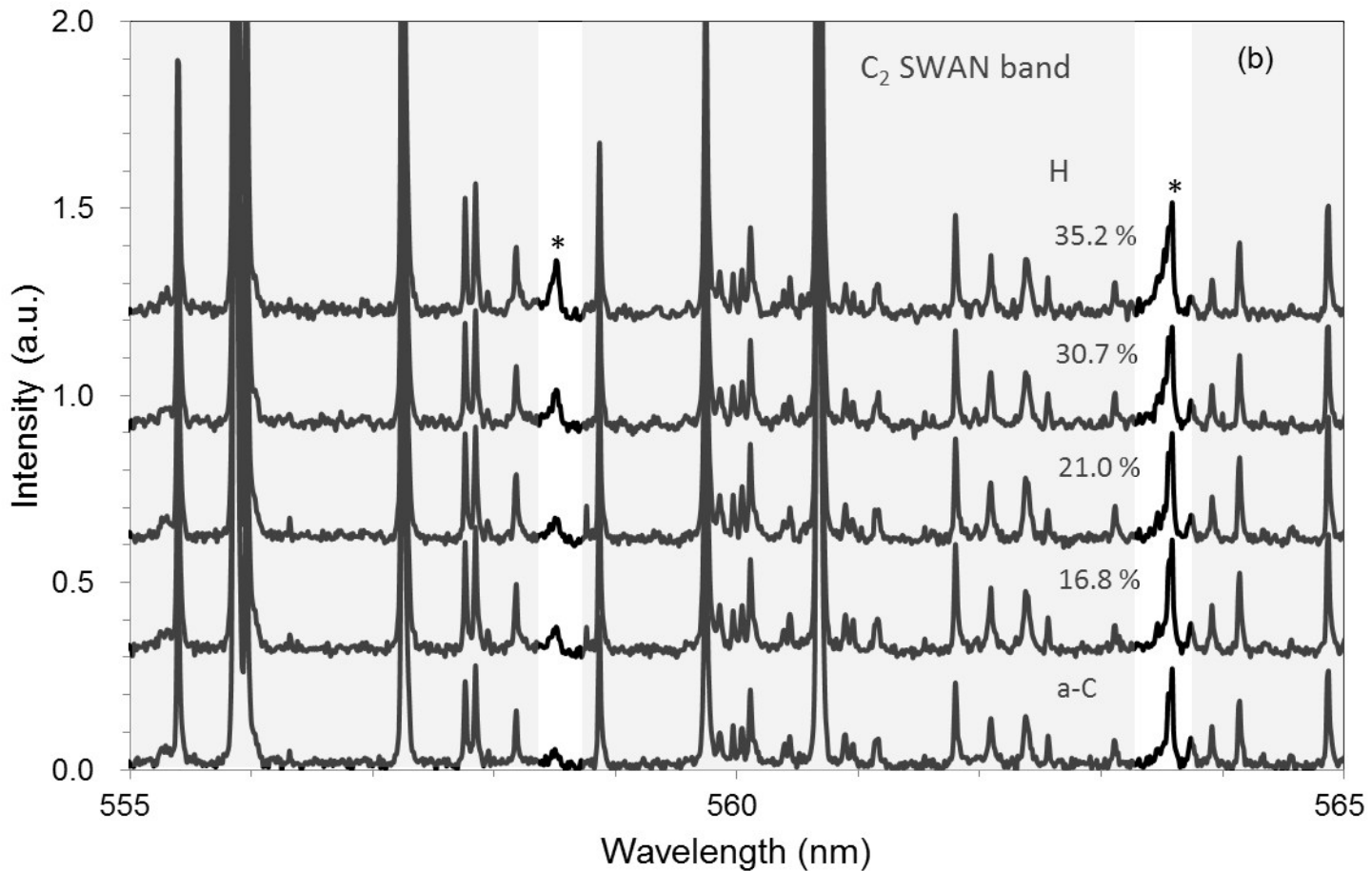
1
2
3
4
5
6
7
8
9
10
11
12
13
14
15
16
17
18
19
20
21
22
23
24
25
26
27
28
29
30
31
32
33
34
35
36
37
38
39
40
41
42
43



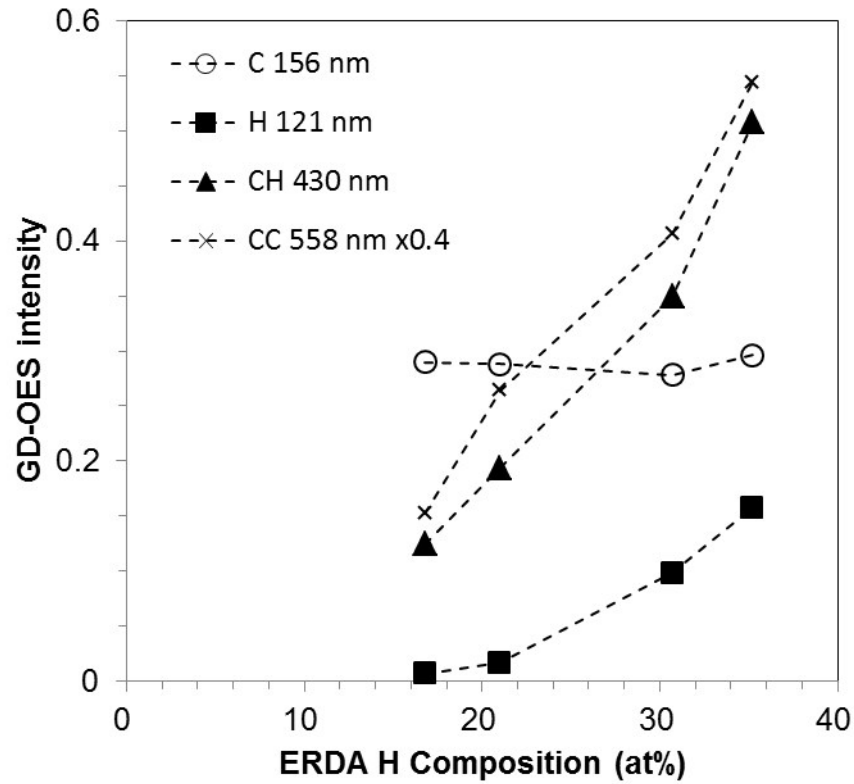
Journal of Analytical Atomic Spectrometry Accepted Manuscript

Fig7

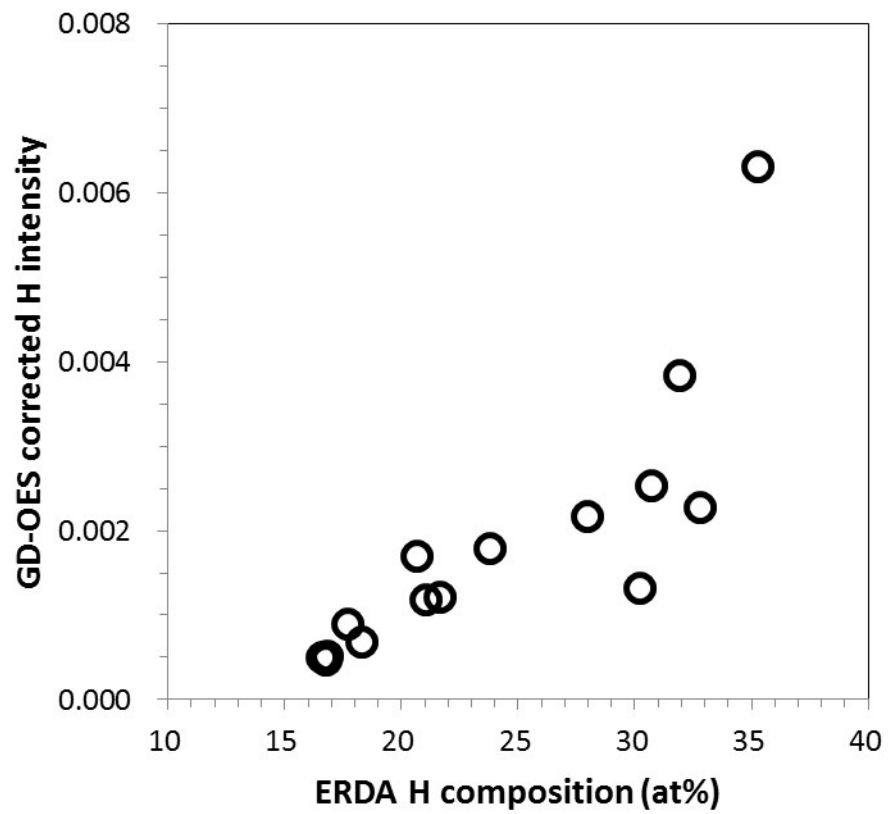




1
2
3
4
5
6
7
8
9
10
11
12
13
14
15
16
17
18
19
20
21
22
23
24
25
26
27
28
29
30
31
32
33
34
35
36
37
38
39
40
41
42
43



1
2
3
4
5
6
7
8
9
10
11
12
13
14
15
16
17
18
19
20
21
22
23
24
25
26
27
28
29
30
31
32
33
34
35
36
37
38
39
40
41
42
43



Journal of Analytical Atomic Spectrometry Accepted Manuscript

Fig10